

# Chapter 5

## A Novel Approach for U-Value Estimation of Buildings' Multi-layer Walls Using Infrared Thermography and Artificial Intelligence



Arijit Sen and Amin Al-Habaibeh

**Abstract** Estimating the U-value of walls of buildings is a key process to evaluate the overall thermal performance. Low U-value in buildings is desired in order to keep heat within the envelop and consume less energy in heating. Addressing the limitations in the currently used U-value estimation techniques, this paper proposes a novel approach for estimating the U-value of the envelop of buildings using infrared thermography and Artificial Neural Network (ANN) with the application of a point heat source. The novel system is calibrated by training the ANN in a lab environment using a wide range of samples with multi-layers to be able to estimate the in situ U-value of walls in real buildings during field work with relatively high accuracy.

**Keywords** U-value · Artificial intelligence · Neural network · Infrared thermography · Insulation

### 5.1 Introduction

The thermal performance of buildings is largely dependent on the thermal transmittance or U-value of their walls. The theoretical U-value of a building's wall is calculated as the reciprocal of the summation of thermal resistance values of different layers of the wall, where thermal resistance is a function of thermal conductivity and thickness of the layers [1].

$$U = \frac{1}{R_i + \frac{d_1}{k_1} + \frac{d_2}{k_2} + \dots + R_e} \quad (5.1)$$

Equation (5.1) represents the theoretical  $U$  value of the wall where,  $k$  is the thermal conductivity of the materials in different layers of the wall,  $d$  is the thickness of the

---

A. Sen (✉) · A. Al-Habaibeh  
Product Innovation Centre (PIC), Nottingham Trent University, Nottingham, UK  
e-mail: [arijit.sen2016@my.ntu.ac.uk](mailto:arijit.sen2016@my.ntu.ac.uk)

A. Al-Habaibeh  
e-mail: [Amin.Al-Habaibeh@ntu.ac.uk](mailto:Amin.Al-Habaibeh@ntu.ac.uk)

wall's layers.  $R_i$  and  $R_e$  are the thermal resistance of air at internal surface and external surface respectively. The U-value of an existing building's wall often differs from its theoretical U-value because of the degradation of the wall materials, deviation of the layers' thicknesses from their designed values, presence of voids between two layers resulting from poor craftsmanship and so on [2]. Also, in some countries the quality of materials used and type are not well-characterised in terms of thermal performance and consistency. There are different approaches exist for determining the U-value of existing buildings; however, they have some limitations [3]. One of the approaches, for example, requires collecting samples of wall materials for laboratory test by drilling holes through walls [3]. Two other non-invasive methods, namely: Heat Flux Meter (HFM) method and Infrared Thermovision Technique (ITT), are limited to be performed in winter only, as they require over 10°C temperature gradient between indoor and outdoor environment [4, 5]. Another approach of estimating U-value from external and internal wall temperatures is by using noncontact infrared sensors; this technique shows better performance over HFM method; however, it is restricted to use during night only and it requires the measurement to be conducted over a few days [6]. The reliable estimation of in situ U-value is difficult in real buildings because of many constraints such as, installing instruments, extended period of monitoring time, dependency on season, dependency on weather condition and presence of sunlight [4–6]. Furthermore, nonlinear and complex relationship among different parameters need to be considered for accurate estimation of U-value. Artificial Neural Network (ANN) could form a very strong tool to analyse nonlinear and complex relationship among input and output parameters and a previous research work shows successful use of infrared thermography and ANN with application of point heat for categorising walls with different U-values [3]. ANN can be trained to learn the relationship between inputs and outputs in a data set and apply the learning process to estimate the outputs from a similar unknown data set. The thermal profile that is generated from infrared images of walls with known U-value can be used to train ANN which later will be able to determine the U-value of an unknown wall. This paper presents a study with a novel product designed to estimate the U-value of a real building's wall from infrared images with application of point heat source using ANN, where the product is calibrated by training the ANN in laboratory environment with different wall samples.

## 5.2 Methodology

Wall sections with different U-values have been monitored with an infrared camera during the application of a point heat in the internal side of the walls. The thermal profiles generated from the monitored infrared images are used as the inputs for the ANN and theoretical U-values of those wall sections as the outputs to train ANN. Later, the thermal response of a real building's wall during the application of a similar point-heat in the internal side of the wall is monitored using infrared camera and the thermal profiles generated from the infrared image are analysed with the

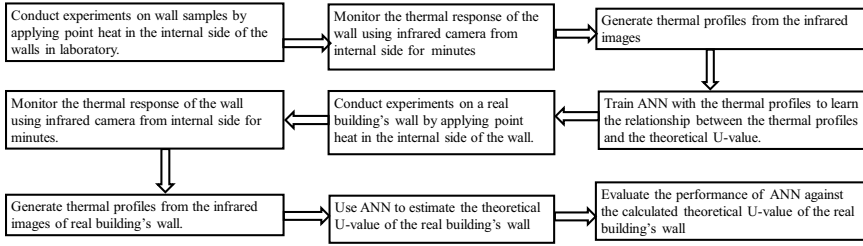


Fig. 5.1 Flow chart of the suggested methodology

ANN to estimate the U-value of the wall. The flow chart in Fig. 5.1 represents the methodology of this study. The ANN performance has been evaluated against the absolute deviation using Eq. (5.2).

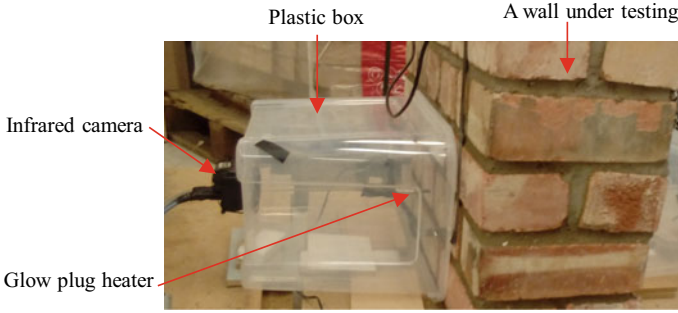
$$\text{Absolute Deviation} = \frac{|U_{\text{predicted}} - U_{\text{calculated}}|}{U_{\text{calculated}}} \times 100\% \tag{5.2}$$

where  $U_{\text{predicted}}$  is the ANN estimated U-value and  $U_{\text{calculated}}$  is the theoretical U-value of real building's wall using Eq. (5.1). The training and evaluation of ANN have been performed 25 times to generalise the solution and the average value of them is considered as final outcome from the ANN.

### 5.3 Experimental Work

In this study six walls, indexed as A, B, C, D, E and F respectively, are monitored using infrared camera with the application of point heat source from internal side. Sample A is a concrete block wall without any internal or external mortar layers. Samples C and E are solid brick walls without any internal or external mortar layers. Samples B and D are concrete block and solid brick walls respectively with external insulation of 100 mm thick Ecotherm. Infrared images are captured using CHINO TP-L0260EN thermal camera at five seconds interval for about an hour resulting in around 720 images per set up of the experiment. Figure 5.2 shows the experimental work on one of the lab samples. The infrared camera is fitted into a plastic box which contains a diesel engine glow plug (Fig. 5.2). The glow plug acts as a point heat source and it is fitted within a plastic box in such a way that it always stays in touch with the internal wall surface. Two K-type thermocouples connected to NIUSB-TC01 data acquisition system are used to measure the glow plug's tip temperature and the ambient temperature respectively.

Experiments on samples A-E are conducted in lab environment and infrared images obtained from the experiments are used for the calibration process by training the ANN. The experiment on sample F is done inside a real building and infrared images captured during the experiment are used to estimate the U-value of the wall



**Fig. 5.2** The setup configuration of the experimental work

with the help of the calibrated ANN. The properties of the wall samples are listed in Table-1, where the U-values are calculated using Eq. (5.1). The values of  $R_i$  and  $R_e$  is taken as 0.13 and 0.04 respectively [7]. The thermal conductivity of concrete block in samples A and B are considered as 1.5 W/mK [8] and the thermal conductivity of the Ecotherm is 0.022 W/mK [9]. The thermal conductivity of brick in samples C and D are taken as 0.27 W/mK [10] and the thermal conductivity of the brick in samples E and F are taken as 0.56 for inner leave and 0.77 for outer leave W/mK [7] as the brick in the samples E and F are different than brick in the samples C and D.

## 5.4 Results and Discussion

Figure 5.3 represents the temperature profile and infrared image of samples D, E and F. It is noted in Fig. 5.3 that sample D has the warmest wall surface. As sample D has the lowest U-value, most of the heat is spread on the wall surface. Sample E has higher U-value than sample F and therefore, sample F is expected to have warmer wall surface. However, the infrared images in Fig. 5.3 convey the opposite information. This is also observed in the temperature profiles in Fig. 5.3.

This could happen due to the difference in ambient temperature during the time of experiments. Previous research work [3] also supports the fact and recommends three modified profiles as presented in Eqs. (5.3), (5.4) and (5.5).

$$T_{(i,j,k)}^a = T_{(i,j,k)} - T_k^{ext} \quad (5.3)$$

$$T_{(i,j,k)}^b = \sum_1^k [T_{(i,j,k+1)} - T_{(i,j,k)}] \quad (5.4)$$

$$T_{(i,j,k)}^{ab} = \sum_1^k [T_{(i,j,k+1)}^a - T_{(i,j,k)}^a] \quad (5.5)$$

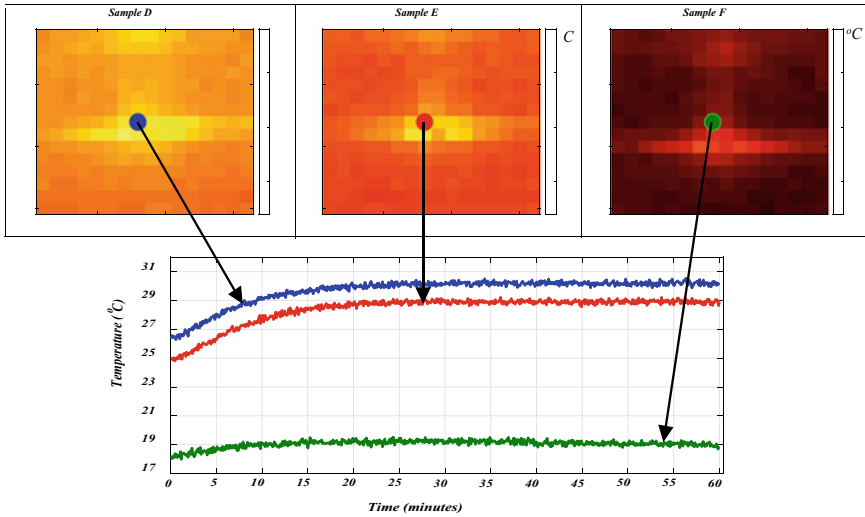



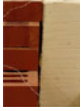




Fig. 5.3 A comparison between temperature profiles: sample D, E and F

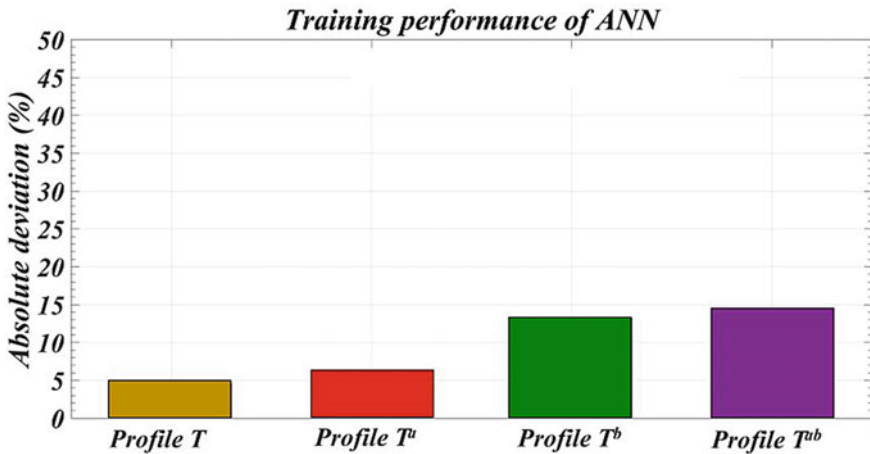
Here  $T_{(i,j,k)}$  is the original temperature value at pixel  $(i,j,k)$  on infrared image,  $T^a_{(i,j,k)}$  is the modified temperature value of pixel  $(i,j,k)$  on the infrared image,  $T^b_{(i,j,k)}$  is the cumulative temperature difference at pixel  $(i,j,k)$ ,  $T^{ab}_{(i,j,k)}$  is the cumulative temperature difference of profile  $T^a$  and  $T^{ext}_k$  is the external temperature at the time of capture of the corresponding infrared image. In Eqs. (5.3) to (5.5),  $i$  and  $j$  refer to the pixel indices of infrared image in x and y direction respectively, and  $k$  refers to the image index in the sequence of infrared images. A feed forward neural network with single hidden layer containing 20 neurons is developed using MATLAB. Sigmoid transfer function is used in the neurons of hidden layer and Levenberg-Marquardt backpropagation algorithm is used as the learning algorithm. The standard deviation of profile  $T$ ,  $T^a$ ,  $T^b$  and  $T^{ab}$  are selected as the input parameters to the neural network and the U-value listed in Table 5.1 as the output. The training data set contains 60 samples of each profile taken equally from the walls AE mentioned in Table 5.1. The test data set is composed of 12 samples from each profile of the wall F. Figure 5.4 shows the average training performance of ANN for profile  $T$ ,  $T^a$ ,  $T^b$  and  $T^{ab}$  of samples A-E. The absolute deviation ranges between 5% to 15% with profile  $T$  having the lowest absolute deviation and profile  $T^{ab}$  having the highest.

Figure 5.5 represents the ANN's performance regarding predicting the U-value of sample F. The theoretical U-values are the target for the ANN and the ANN predicted U-values are the achievement made. The bar chart in Fig. 5.5a compares the performance of ANN with the target values. It is found in Fig. 5.5a, that the ANN produces the closest prediction to the theoretical U-value in profile  $T^b$ . Profile  $T^b$  and  $T^{ab}$  achieve the lowest absolute deviation which is around 20% (Fig. 5.5b). The training performance of ANN for profile  $T$  is found to be the best but the test performance is the worst among all profiles, which indicates that ANN overfits this

**Table 5.1** Properties of wall samples used to train and test ANN

Sample Number	Training Samples					Test Sample
	A	B	C	D	E	F
Material	Concrete block wall	Concrete block + External insulation with Ecotherm	Brick	Brick + External insulation with Ecotherm	Solid Brick Wall	Inner mortar layer + Solid Brick Wall + Outer mortar layer
Thickness (mm)	95	95 + 100 = 195	100	100 + 100 = 200	230	15 + 230 + 20 = 265
Thermal Conductivity (W/mK)	1.5	1.5 & 0.22	0.27	0.27 & 0.22	0.56* & 0.77**	0.88, 0.56, & 0.94 respectively.
U-value (W/m <sup>2</sup> K)	4.29	1.45	1.86	1.01	1.92	1.62
Cross section						

\*Inner layer, \*\*Outer layer



**Fig. 5.4** Average training performance of ANN for different profiles of samples A-E

profile. On the other hand, the difference between the training performance and the test performance are found to be the lowest for profile T<sup>ab</sup>, which indicates the best fit among all profiles. Similarly, for profile T<sup>b</sup>, ANN shows a reasonable difference between training performance and test performance indicating a better fit

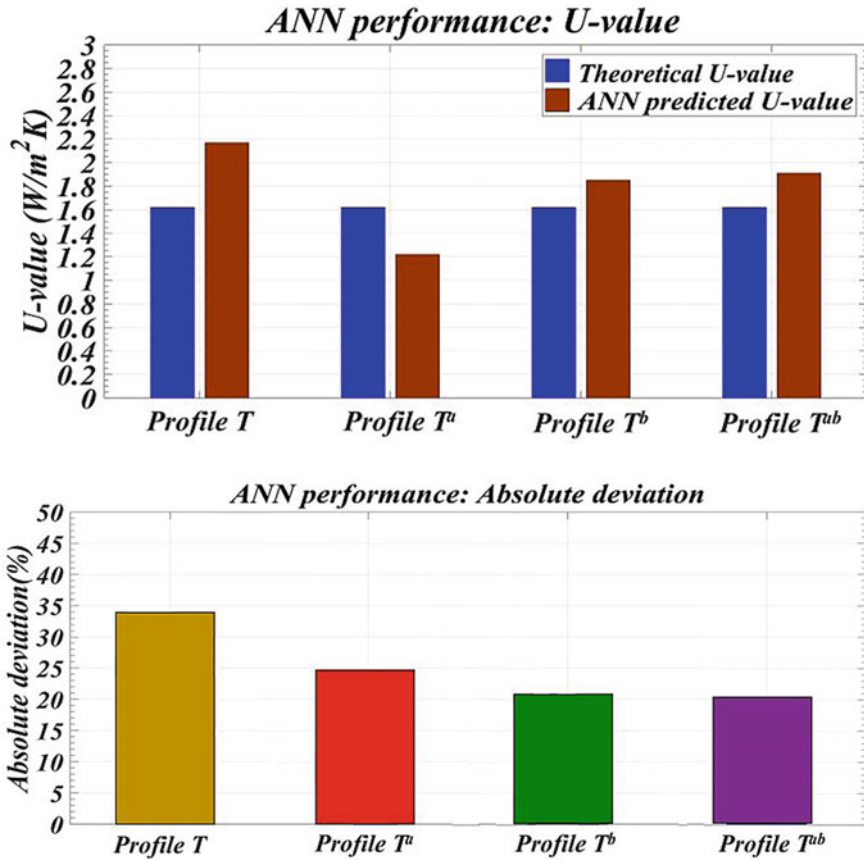


Fig. 5.5 a A comparison between theoretical and predicted U-values; b The absolute deviations of different profiles

than the two others. In profile  $T^a$ , the difference between training performance and test performance is significantly high indicating an overfit as well. The profiles  $T^{ab}$  and  $T^b$  are developed considering the cumulative temperature difference; and thus, it generalises the thermal behaviour of walls more precisely. As a result, the ANN produces the best performance for those two profiles.

### 5.5 Conclusion

The U-value of buildings' walls signifies the thermal performance and the energy transferred via the envelop. There is a need to estimate the U value of buildings' components in situ and in a rapid way. This paper presents a novel approach of

determining U-value of a real building's wall by designing a novel product that can be calibrated using the training process of an ANN with the help from material samples in the lab. The results signify the ability of ANN to estimate U-value of real building based on the analysis of infrared data captured during the application of a point heat. There is no general rule to decide on the optimum configuration of an ANN or the most efficient size of training data set required to perform successful ANN analysis; as this depends on the nature of the utilised data as input and target values. The results presented in this paper show that ANN is capable of estimating U-value of buildings' wall with 80% accuracy, including multi-layered walls. Future work will be utilised to attempt to enhance the accuracy of the system using other ANN architectures, including more training data, and compare between the existing technologies and the this suggested one.

## References

1. K. Gaspar, M. Casals, M. Gangoellis, A comparison of standardized calculation methods for in situ measurements of façades U-value. *Energy Build.* **130**, 592–599 (2016)
2. L. Evangelisti et al., In situ thermal transmittance measurements for investigating differences between wall models and actual building performance. *Sustainability* **7**(8), 10388–10398 (2015)
3. A. Sen, A. Al-Habaibeh, The design of a novel approach for the assessment of thermal insulation in buildings using infrared thermography and artificial intelligence. *Int. J. Design Eng.* **9**(1), 65–77 (2019)
4. G. Ficco et al., U-value in situ measurement for energy diagnosis of existing buildings. *Energy Build.* **104**, 108–121 (2015)
5. R. Albatici, A.M. Tonelli, M. Chiogna, A comprehensive experimental approach for the validation of quantitative infrared thermography in the evaluation of building thermal transmittance. *Appl. Energy* **141**, 218–228 (2015)
6. N. Sakkas et al., Non intrusive U value metering. *Open J. Energy Effic.* **4**, 28–35 (2015)
7. B. Anderson, Conventions for U-value calculations 2006 Edition UK: BRE Press Scotland (2006)
8. ISO FDIS 10456 (2007) Building materials and products—Hygrothermal properties—Tabulated design values and procedures for determining declared and design thermal values. <http://www.superhomes.org.uk/wp-content/uploads/2016/09/Hygrothermal-properties.pdf>. Accessed May 14, 2018
9. EcoTherm Rigid Thermal Insulation Boards. <https://www.ecotherm.co.uk/about-us/features-benefits>. Accessed April 29, 2019
10. K.D. Antoniadis, M.J. Assael, C.A. Tsiglifisi, S.K. Mylona, Improving the design of greek hollow clay bricks. *Int. J. Thermophys.* **33**(12), 2274–2290 (2012)



**Open Access** This chapter is licensed under the terms of the Creative Commons Attribution 4.0 International License (<http://creativecommons.org/licenses/by/4.0/>), which permits use, sharing, adaptation, distribution and reproduction in any medium or format, as long as you give appropriate credit to the original author(s) and the source, provide a link to the Creative Commons license and indicate if changes were made.

The images or other third party material in this chapter are included in the chapter's Creative Commons license, unless indicated otherwise in a credit line to the material. If material is not included in the chapter's Creative Commons license and your intended use is not permitted by statutory regulation or exceeds the permitted use, you will need to obtain permission directly from the copyright holder.

